The Shielding Constants and Scalar Couplings in N−H···O=C and N−H···N=C Hydrogen Bonded Systems: An ab Initio MO Study

Magdalena Pecul,*,†,‡ Jerzy Leszczynski,† and Joanna Sadlej‡

Computational Center for Molecular Structure and Interactions, Department of Chemistry, Jackson State University, Jackson, Mississippi 39217, and Department of Chemistry, University of Warsaw, Pasteura 1, 02−093 Warsaw, Poland

Received: March 31, 2000; In Final Form: June 13, 2000

The scalar spin−spin coupling constants, both intra- and intermolecular, were evaluated for the models of biological systems: formamide−formamide (Fa−Fa) and formamide−formamidine (Fa−Fi) dimers using the MCSCF method. Additionally, the shielding constants were calculated at the MCSCF and MP2 levels. ^{1}J(NH) and ^{2}J(NH) couplings are the most significantly affected by the hydrogen bond formation. The hydrogen-bond transmitted coupling constants ^{1h}J(NH) and ^{2h}J(NN) calculated for the Fa−Fi dimer are in agreement with recent experimental results for nucleic acids. The short-distance hydrogen-bond-transmitted couplings (e.g., ^{1h}J(NH) and ^{2h}J(NN)) decrease fast with increase in the hydrogen bond length, in contrast to the long-distance proton−proton intermolecular couplings. The changes in the shieldings of the protons engaged in the hydrogen bond formation and proton acceptors are found to decrease fast with increase in the hydrogen bond length, in accordance with the previous results.

Introduction

The characterization of hydrogen bonding is one of the basic problems of theoretical and experimental chemistry. The hydrogen bonding has been extensively investigated[1,2] as a determinant of the spacial structure of biopolymers, and, recently, as a possible factor in enzymatic catalysis.[3−7] NMR spectroscopy is indispensable for detection and characterization of the hydrogen bonds, particularly for large systems of biochemical interests. Until recently, mostly the chemical shifts,[8−11] anisotropies of the chemical shifts,[10,12] and nuclear quadrupole coupling constants[10,13] have been used for this purpose. The progress in the NMR spectroscopy has now made it possible to use also the nuclear spin−spin coupling constants as the hydrogen bond parameters.[14−22] An advancement in this field has been made by measurements of the interresidual hydrogen-bond-transmitted coupling constants,[15−23] which provide unique direct experimental evidence for the formation of the hydrogen bond, usually detected through changes in some properties of monomers (e.g., IR frequencies and intensities or NMR shieldings).

The ab initio calculations of the spin−spin coupling constants require the use of sophisticated computational techniques including the electron correlation effects[24,25] and are very time-consuming. In contrast, NMR shielding constants can be calculated with acceptable accuracy at the SCF level.[24,26] As a result, the ab initio calculations of the spin−spin coupling constants in hydrogen-bonded systems are still not widespread, while the changes of the shielding constants caused by the formation of hydrogen bonding have been frequently investigated by means of ab initio calculations[8,11,27−31] (see refs 24 and 32 for review).

As a consequence of the above and since the measurements of the interresidual couplings are only a recent achievement,[15−23] the theoretical calculations of these properties are scarce.[20,21,33−37] The couplings through N−H···O=C and N−H···N=C hydrogen bonds were evaluated[20,34,37] in only three papers. These calculations employed the density functional method (DFT). DFT usually performs satisfactorily (and in some cases surprisingly well)[38,39] for the couplings involving protons and carbons. However, the performance of DFT rapidly deteriorates with the number of lone pairs borne by the coupled nuclei,[39] so for the couplings involving N, O, and F it is not reliable, as the example of $(HF)_n F^-$ complexes indicates.[21,34] Moreover, in the previous studies the spin-dipole (SD) term was neglected and in ref 20 only the Fermi contact (FC) term was calculated. The noncontact contributions are in fact in many cases small but by no means negligible, especially the diamagnetic and paramagnetic spin−orbit (DSO and PSO) terms. In addition, omission of the SD term may lead to considerable errors, as is indicated by the examples of CO and N_2.[40] In calculations of new types of couplings it would be advisable to evaluate all four contributing terms, particularly in view of the existing controversy concerning the character of the hydrogen-bond-transmitted couplings and the hydrogen bonding.[41]

In the present study, the spin−spin coupling constants and the NMR shielding constants are evaluated for the hydrogen bonded formamide−formamide (Fa−Fa) and formamide−formamidine (Fa−Fi) complexes by using molecular orbital methods including electron correlation effects. The Fa−Fa complex was chosen as a model of hydrogen bonding in peptides, while the Fa−Fi complex serves as a model of interaction between the complementary pairs of nucleic basis (adenine−thymine in DNA or adenine−uracil in RNA).[42−44] The limitations of the applied computational methods are considered and the possible sources of errors are discussed.

The paper is organized as follows: In the section titled Computational Method the computational methods employed for geometric optimization of the complexes and calculations of the NMR parameters are described. Later, the methodological

* Corresponding author. E-mail: magda@joanna.chem.uw.edu.pl.
† Jackson State University.
‡ University of Warsaw.

10.1021/jp001251x CCC: $19.00
Published on Web 08/08/2000

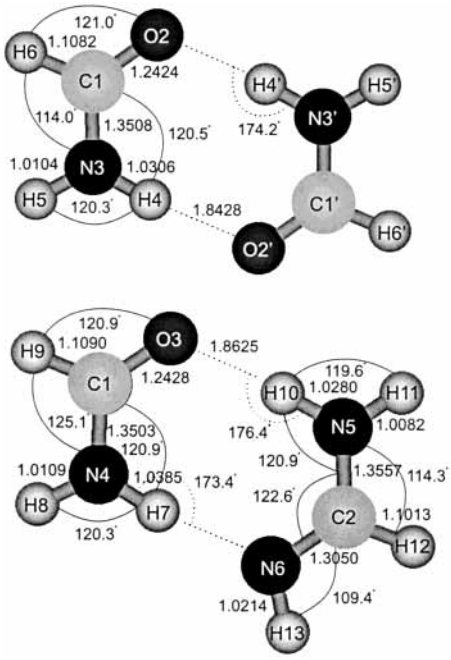

Figure 1. The optimized geometry parameters (bond distances in angstroms, bond angles in degrees) of Fa−Fa dimer and Fa−Fi dimer.

aspects and the computational accuracy of the NMR parameters calculations are discussed on the basis of the results for Fa and Fi monomers (the section titled Quality of the Results). Next, in the section titled **NMR Parameters in Optimized Fa−Fa and Fa−Fi Complexes**, the calculated complexation-induced changes of the isotropic and anisotropic shielding constants (the subsection titled *Changes of the Shielding Constants*) and those of the intramolecular spin−spin coupling constants (the next subsection) are presented. In the last part of this section we analyze the hydrogen-bond-transmitted couplings in Fa−Fa and Fi−Fa complexes. The dependence of the above parameters on the hydrogen bond length is then discussed in the section titled **Dependence of the NMR Parameters on the Hydrogen Bond Length**. Finally, a summary and main conclusions are presented.

Computational Method

The Fa−Fa and Fa−Fi complexes were subjected to the MP2-(frozen core)/aug-cc-pVDZ geometry optimization starting from the structures described in refs 42 and 43. The geometry parameters of the monomers were also optimized at the same level. To preserve the resemblance to the peptides and nucleic basis, the monomer geometries were assumed to be planar during the optimization, which seems to correspond to the actual structure of formamide.[45] The resulting optimized structures of the Fa−Fa and Fa−Fi complexes are visualized in Figure 1. The interaction energies calculated for the optimized structures are counterpoise corrected[46] and include the monomer deformation effects.[47]

The scalar spin−spin coupling constants and the NMR shielding constants were calculated for the optimized structures of Fa, Fi monomers and Fa−Fa, Fa−Fi complexes. The NMR shielding constants were calculated at the MP2(all-electron)/aug-cc-pCVDZ level by using gauge including atomic orbitals (GIAO). Additionally, the MP2(all-electron)/cc-pCVTZ and MP2(all-electron)/cc-pCVDZ calculations of the shielding constants were carried out for Fa and Fi monomers. The geometry optimization and the MP2 calculations of the NMR shielding constants were performed by using the GAUSSIAN98 software.[48] The NMR shielding constants were also calculated by means of the MCSCF method described below.

The scalar spin−spin coupling constants were calculated by using the linear response MCSCF method[24,49] implemented in the Dalton software.[50] All four terms contributing to the isotropic couplings were calculated, unless noted otherwise. In Dalton the DSO contribution is evaluated as an expectation value, while the other contributions are calculated as response properties. The following restricted active space (RAS) wave function models were used for the dimers: (8/-/16/18 *2e*) for Fa−Fa and (7/-/17/18 *2e*) for Fa−Fi, where numbers in parentheses correspond to numbers of orbitals in the inactive, RAS1, RAS2, and RAS3 spaces, respectively, and maximum 2 electrons are excited to RAS3 space. The active spaces were chosen on the basis of the MP2 occupation numbers. In each wave function the core 1s orbitals of C, N, and O atoms and the lowest valence orbitals (corresponding to 2s O orbitals) were kept inactive. Since we are not particularly interested in practically unmeasurable couplings involving oxygen nuclei, this simplification should not introduce any major errors. In the additional calculations for the monomers the (3/-/9/19 *2e*) RAS wave function denoted RAS3 in ref 45 was used. The basis set employed in the calculations of spin−spin coupling constants is aug-cc-pVDZ-su-1 for all atoms except carbons, for which, for computational reasons, the cc-pVDZ-su-1 basis set was used. The lack of diffuse functions on the carbon atoms does not impair the computed coupling constants, as our preliminary calculations showed. The medium-size aug-cc-pVDZ-su-1 basis set is constructed from the standard cc-pVDZ basis set of Dunning[51] by augmentation by diffuse functions,[52] decontraction of s orbitals, and addition of one tight s orbital.[36,53] As a result, it contains both a large number of s functions, essential for the calculation of the coupling constants, and the diffuse orbitals required for the proper description of the intermolecular interactions. For the monomers, additional calculations were performed in the larger cc-pVTZ-su-1 basis set (constructed analogously to aug-cc-pVDZ-su-1) and the cc-pVDZ-su-1 basis set to estimate the errors resulting from the basis set incompleteness.

The calculations of the changes in the molecular properties resulting from the formation of strongly interacting complexes require taking into account both the counterpoise correction and the monomer relaxation effects. This can be done straightforwardly for size-consistent MP2 calculations of the shielding constants but is more problematic for nonsize-consistent calculations of the coupling constants with RAS wave function. This latter problem is bypassed by the estimation of the counterpoise correction at the SCF level and calculation of the monomer relaxation effect by means of RAS3 wave function, i.e., on a different level than the complexation-induced change itself. This approach was also applied in our other studies[35,36] and seems to be justified.

Apart from the calculations for the optimized complex geometries, the NMR shielding constants and the hydrogen bond-transmitted spin−spin coupling constants in Fa−Fa and Fa−Fi were evaluated for four other intermolecular distances, to establish their dependence on the hydrogen bond length.

Results and Discussion

Quality of the Results. In this section the influence of the electron correlation and the basis set effects on the calculated NMR shielding constants and the spin−spin coupling constants are discussed on the basis of the results for Fa and Fi monomers. The internal monomer geometries of the Fa−Fa and Fa−Fi

TABLE 1: The Calculated Isotropic Shielding Constants (in Parts per Million) in Formamide (Fa) and Formamidine (Fi) Monomers with Dimerlike[a] Geometry

	SCF/aug-cc-pCVDZ	MP2/aug-cc-pCVDZ	RAS3/aug-cc-pCVDZ	MP2/cc-pCVDZ	MP2/cc-pCVTZ	exp[b]
			^{1}H[c] shielding			
Fa	26.1	26.0	26.1	26.8	26.1	23.79−23.68
Fi	26.5	26.4	26.5	27.3	26.5	
			^{17}O shielding			
Fa	−68.7	−16.2	−7.4	−42.0	−65.0	39.06−36.3
			^{15}N shielding			
Fa	170.1	179.1	183.0	184.1	168.6	131.6−131.4
Fi (−NH_2)	193.5	201.3	205.4	207.7	193.4	
Fi (−NH)	33.6	72.6	68.1	67.0	45.9	
			^{13}C shielding			
Fa	25.9	48.7	36.3	56.6	34.3	23.37−24.19
Fi	30.7	54.7	42.5	61.4	40.3	

[a] Geometry parameters of Fa−Fa dimer for Fa and of Fa−Fi dimer for Fi. [b] Liquid-phase experimental data from ref 45. [c] Only the shielding of ^{1}H engaged in hydrogen bond formation in the dimers given.

dimers are employed to facilitate the comparison with subsequently discussed NMR parameters of the dimers.

Shielding Constants. The isotropic shielding constants calculated for the formamide and formamidine monomers are tabulated in Table 1. Only the shielding constants of the atoms participating in the hydrogen bond formation are referred to since only the quality of these results is of interest in the further studies. The same procedure is followed later for the spin−spin coupling constants. Our presentation of the shielding constants is limited here to the isotropic shieldings since the trends for the shielding anisotropies are parallel.

(a) Electron Correlation Effects. The comparison of the shielding constants of formamide with experiment[45] suggests that the reported MP2 results are fairly accurate. The exception is σ (^{17}O) for which the inclusion of the correlation effects diminishes the discrepancy with liquid-phase experiment but does not eliminate it. The explanation of this fact lies probably in the very large effects of the hydrogen bond formation on the ^{17}O shielding (see below). The inclusion of this effect in the calculations for the formamide dimer improves considerably the agreement with experiment. The most significant differences between SCF and MP2 results (columns 1 and 2 of Table 1) emerge for the shieldings of nuclei bound by (formally) multiple bonding: σ (^{17}O) and σ (^{13}C) in C═O group of formamide, σ (^{15}N) and σ (^{13}C) in the C═N−H group of formamidine. The MCSCF results for these shieldings are similar to the MP2 ones, but on the whole the MCSCF results are closer to the experimental data.

Since the MP2 method is known to overestimate the electron correlation effects on the shielding constants[24] in such systems as those under study, for the hydrogen bond-induced changes of the shielding constants discussed subsequently in the paper the SCF and MCSCF results are also given. In principle MCSCF should be a better method for the calculations of the shielding constants in multiple bound atoms than the MP2 method. However, the lack of size consistency in MCSCF makes the MP2 method preferable for the calculations of the effects of complexation.

(b) Basis Set Effects. The comparison of the shielding constants calculated with the aug-cc-pCVDZ and cc-pCVTZ basis sets indicate that the former is far from being complete, although it improves significantly on cc-pCVDZ. The ^{1}H, ^{13}C, and ^{15}N shieldings in amino groups calculated in the aug-cc-pCVDZ and cc-pCVTZ basis sets are in reasonable agreement. Still, σ (^{17}O) in C═O group of formamide and σ (^{15}N) in C═N−H group of formamidine are very discrepant and it seems that the extension of the basis set would be advisable. However, the size of the Fa−Fa and Fa−Fi dimers precludes the MP2 GIAO calculations of the shielding constants with significantly larger basis sets.

Notably, the ^{17}O shielding constant calculated on the MP2 level with the larger cc-pCVTZ basis sets is more discrepant with experiment[45] than that obtained with the smaller aug-cc-pCVDZ basis set, in contrast to the other shieldings for which the results obtained by using cc-pCVTZ are in better agreement with existing experimental data.[45] The reason for this discrepancy is the large influence of the hydrogen bonds on this shielding.

Spin−Spin Coupling Constants. The selected spin−spin coupling constants calculated for formamide and formamidine monomers with the dimer-like geometries are presented in Table 2. These data enable us to assess the errors resulting from the simplifications necessary for the calculations on Fa−Fa and Fa−Fi dimers. More specifically, the comparison of RAS^{dim} (RAS space used for the calculations for the complex) and RAS3 results serves as an estimation of the electron correlation effects not included in RAS^{dim}. The comparison of aug-cc-pVDZ-su-1, cc-pVDZ-su-1, and cc-pVTZ-su-1 results gives the information on the incompleteness of the aug-cc-pVDZ-su-1 basis set.

(a) Electron Correlation Effects. The differences between RAS^{dim} and RAS3 results are more substantial for the couplings between heavier atoms than for the proton−proton couplings. The largest relative discrepancy between RAS^{dim} and RAS3 is observed for ^{1}J(CO) in formamide. It probably originate from noninclusion of the forth lowest molecular orbital (localized predominantly on O) in the RAS^{dim} active space. The RAS^{dim} and RAS3 results for the other couplings are similar and agree with experiment, which indicates that the errors for the dimers should not be large.

(b) Basis Set Effects. Contrary to what was observed for the shielding constants, the effects of the basis set incompleteness on the spin−spin coupling constants are not significant. The couplings involving heavier nuclei are practically basis-set independent and for ^{3}J(HH) couplings the discrepancies between aug-cc-pVDZ-su-1 and cc-pVTZ-su-1 do not exceed 10%. The cc-pVDZ-su-1 results are more discrepant with the cc-pVTZ-su-1 ones, which indicates that the diffuse functions in aug-cc-pVDZ-su-1 not only are necessary for the calculations on the interacting molecules but improve the description of the valence shell. The errors resulting from lack of diffuse functions on C atoms are negligible, as is indicated by the results of our additional calculations.[54] This suggests that the calculations for the dimers should be reasonably accurate as far as the basis set is concerned.

TABLE 2: The Calculated Spin−Spin Coupling Constants (in Hertz) in Formamide (Fa) and Formamidine (Fi) Monomers with Dimerlike[a] Geometry

	RAS[dim]/aug-cc-pVDZ-su-1	RAS3/aug-cc-pVDZ-su-1	RAS3/cc-pVDZ-su-1	RAS3/cc-pVTZ-su-1	exp.[b]	exp.[c]
			^{1}J(NH) coupling			
Fa ^{1}J(N3H4)	−94.4	−91.2	−90.9	−94.5	−88.68	−86.9 − −87.8
Fa ^{1}J(N3H5)	−91.5	−89.4	−88.5	−92.3	−91.49	−90.3 − −92.0
Fi ^{1}J(N5H10)	−96.2	−92.6	−92.4	−96.0		
Fi ^{1}J(N5H11)	−94.5	−91.4	−90.6	−94.5		
Fi ^{1}J(N6H13)	−61.1	−57.0	−52.6	−57.5		
			^{1}J(CO) coupling			
Fa ^{1}J(C1O2)	19.3	24.3	26.5	25.2		
			^{1}J(CN) coupling			
Fa ^{1}J(C1N3)	−21.1	−18.9	−19.3	−19.2	−14.82	−19.5 − −20.8
Fi ^{1}J(C2N5)	−27.0	−24.2	−25.0	−24.4		
Fi ^{1}J(C2N6)	−14.3	−10.2	−9.1	−9.6		
			^{1}J(CH) coupling			
Fa ^{1}J(C1H6)	212.7	190.9	187.0	196.2	193.11	183.6 − 192.8
Fi ^{1}J(C2H12)	173.5	171.8	167.0	176.2		
			^{2}J(NH) coupling			
Fa ^{2}J(N3H6)	−16.8	−16.4	−16.8	−17.2	−13.49	−14.3 − −18.9
Fi ^{2}J(N5H12)	−8.5	−9.2	−9.4	−9.7		
Fi ^{2}J(N6H12)	5.8	5.0	4.2	4.7		
			^{3}J(HH) coupling			
Fa ^{3}J(H6H4)	13.0	12.0	11.8	13.4	13.9	12.9 − 13.9
Fa ^{3}J(H6H5)	1.1	1.1	1.0	1.1	2.25	2.1 − 2.3
Fi ^{3}J(H12H10)	11.7	11.8	11.4	13.1		
Fi ^{3}J(H12H11)	2.5	2.5	2.4	2.7		
Fi ^{3}J(H13H12)	13.1	11.6	11.6	12.5		

[a] Geometry parameters of Fa−Fa dimer for Fa and of Fa−Fi dimer for Fi. [b] Liquid-phase experimental data from ref 45. [c] Earlier liquid-phase experimental data quoted from ref 45.

NMR Parameters in Optimized Fa−Fa and Fa−Fi Complexes. In this section, the results of the calculations of the NMR properties for the optimized Fa−Fa and Fa−Fi complexes are presented. First, the complexation-induced changes of the NMR shielding constants are considered, together with the discussion of the monomer relaxation effects, counterpoise corrections, and electron correlation effects on these properties. Next, the changes of the intramolecular spin−spin coupling constants are examined, also with consideration of the methodological aspects of the calculations. Finally, the hydrogen-bond transmitted spin−spin coupling constants are presented.

Changes of the Shielding Constants. The changes in the NMR shielding constants of the nuclei participating in the hydrogen bonds formation are presented in Table 3 (isotropic shieldings) and Table 4 (shielding anisotropies). The counterpoise-corrected contributions due to the deformation of the electron density $\Delta(\sigma)_{cc}$ and the contributions from the geometry changes accompanying the dimer formation $\Delta(\sigma)_{relax}$ are listed separately for a better insight into the mechanism of the changes. For the comparison, the total shielding changes obtained at the SCF and MCSCF levels are included in Table 3 and Table 4, in addition to the MP2 values.

The changes in the isotropic shielding constants of the protons engaged in the hydrogen bond formation and the proton donors seem to depend predominantly on the type of the proton acceptor. The relevant ^{1}H and ^{15}N isotropic shieldings change similarly in Fa−Fa and Fa−Fi dimers when the oxygen atom of the carbonyl group is the proton acceptor, the type of the donor notwithstanding. The hydrogen bond formation also influences the ^{13}C shielding in Fa and Fi similarly even though the carbon atom is bound differently in these two molecules. Not surprisingly, the changes in the ^{17}O isotropic shielding and shielding anisotropy are alike in Fa−Fa and Fa−Fi dimers, since both proton donor and proton acceptor are practically the same.

(a) Monomer Relaxation and Counterpoise Correction Effects. The monomer relaxation does not contribute significantly to the total changes of the isotropic shielding constants (Table 3). This contribution is practically negligible for the isotropic shielding constants of the proton, of the proton acceptor atom, and of the proton donor atom. It is relatively more important for the small changes of the ^{13}C isotropic shielding.

TABLE 3: The Calculated Changes in the Isotropic Shielding Constants (in Parts per Million) upon Fa−Fa and Fa−Fi Dimer Formation

		$\Delta(\sigma)_{cc}$	$\Delta(\sigma)_{relax}$	$\Delta(\sigma)_{total}$	$\Delta(\sigma)_{total}$ SCF	$\Delta(\sigma)_{total}$ RAS[a]
			^{1}H[b] shielding			
Fa−Fa	Fa	−4.8	−0.7	−5.5	−5.6	−5.5
Fa−Fi	Fa	−6.1	−0.9	−7.0	−7.1	−7.1
Fa−Fi	Fi	−4.7	−0.6	−5.2	−5.3	−5.3
			^{1}H acceptor shielding (^{17}O or ^{15}N)			
Fa−Fa	Fa(O)	42.0	−5.8	36.2	58.0	44.3
Fa−Fi	Fa (O)	41.8	−6.1	35.7	56.0	39.9
Fa−Fi	Fi (N)	23.2	−2.5	20.7	31.7	23.8
			^{1}H donor shielding (^{15}N)			
Fa−Fa	Fa	−16.4	0.3	−16.1	−15.1	−14.2
Fa−Fi	Fa	−21.0	−0.2	−21.2	−19.7	−18.0
Fa−Fi	Fi	−15.4	0.2	−15.2	−14.6	−14.0
			^{13}C shielding			
Fa−Fa	Fa	−4.6	−1.7	−6.3	−6.0	−6.2
Fa−Fi	Fa	−4.5	−1.8	−6.2	−6.0	−5.8
Fa−Fi	Fi	−4.5	−0.8	−5.3	−5.4	−6.0

[a] Not counterpoise corrected. [b] Only the shielding of ^{1}H engaged in hydrogen bond formation in the dimers given.

The hydrogen bond-induced changes in the shielding anisotropy are dominated by the electronic effect for the proton shielding and proton acceptor shielding. However, the monomer relaxation contributes significantly to the changes of the proton donor shielding anisotropy and to the changes of ^{13}C shielding anisotropy.

The counterpoise corrections for the aug-cc-pCVDZ basis set are small even for ^{13}C and ^{17}O shieldings, more susceptible to

TABLE 4: The Calculated Changes in the Shielding Constant Anisotropies (in Parts per Million) upon Fa−Fa and Fa−Fi Dimer Formation

		$\Delta(\Delta\sigma)_{cc}$	$\Delta(\Delta\sigma)_{relax}$	$\Delta(\Delta\sigma)_{total}$	$\Delta(\Delta\sigma)_{total}$ SCF	$\Delta(\sigma)_{total}$ RAS[a]
		^{1}H[b] shielding anisotropy				
Fa−Fa	Fa	9.4	−0.2	9.2	9.0	9.4
Fa−Fi	Fa	12.2	−0.2	12.0	11.5	12.0
Fa−Fi	Fi	9.8	0.0	9.8	9.6	9.9
		^{1}H acceptor shielding anisotropy (^{17}O or ^{15}N)				
Fa−Fa	Fa	−68.8	0.0	−68.7	−103.6	−69.4
Fa−Fi	Fa (O)	−68.1	−1.0	−69.1	−100.8	−61.5
Fa−Fi	Fi (N)	−37.2	−0.4	−37.6	−53.9	−37.4
		^{1}H donor shielding anisotropy (^{15}N)				
Fa−Fa	Fa	−9.3	−5.5	−14.8	−12.9	−12.9
Fa−Fi	Fa (N)	−7.4	−5.8	−13.2	−13.5	−13.2
Fa−Fi	Fi (N)	−13.5	−6.0	−19.6	−16.8	−15.6
		^{13}C shielding anisotropy				
Fa−Fa	Fa	4.4	3.0	7.4	8.3	8.5
Fa−Fi	Fa	3.4	2.6	6.0	7.3	6.7
Fa−Fi	Fi	2.4	2.2	4.6	6.7	8.3

[a] Not counterpoise corrected. [b] Only the shielding of ^{1}H engaged in hydrogen bond formation in the dimers given.

BSSE than ^{1}H shieldings.[30] In contrast to what was found for the interaction energies, the counterpoise corrections for the shielding constants are of the same order of magnitude at the SCF and MP2 levels.

(b) Importance of the Electron Correlation. Comparison of the changes in the shielding constants calculated at the SCF and MP2 levels leads to similar conclusions as for the absolute shieldings in the monomers: Electron correlation influences most significantly the changes in the shieldings (both iso- and anisotropic) of multiply bound atoms, here acting as proton acceptors. These changes are considerably larger when calculated at the SCF level. The complexation-induced changes of the proton acceptor shielding constants calculated at the MCSCF level are larger than the MP2 results but are close to them. We conclude, therefore, that the MP2 results, although slightly underestimated, are reliable.

The changes in the isotropic shielding constants and shielding anisotropies of the remaining nuclei are practically unaffected by the electron correlation. It is particularly gratifying in the case of the proton shieldings since it confirms the validity of the conclusions drawn from numerous SCF calculations of the proton shielding constants in hydrogen bonded systems.[27−29,55]

Changes of the Intramolecular Spin−Spin Coupling Constants. The changes in the selected intramolecular spin−spin coupling constants due to the hydrogen bond formation are tabulated in Table 5. They are discussed below in the following order: first, the one-bond ^{1}J(NH), ^{1}J(CN), ^{1}J(CO), and ^{1}J(CH) couplings; next, the geminal ^{2}J(NH) couplings; and finally the vicinal ^{3}J(HH) couplings.

There are three types of ^{1}J(NH) couplings in the complexes under study: the couplings through the bonds participating in the hydrogen bonding (^{1}J(N3H4) in Fa−Fa, ^{1}J(N4H7), ^{1}J(N5H10) in Fa−Fi), the couplings through adjacent bonds (^{1}J(N3H5) in Fa−Fa, ^{1}J(N4H8), ^{1}J(N5H11) in Fa−Fi), and the coupling of the proton acceptor nitrogen ^{1}J(N6H13) in Fa−Fi. The coupling constants of the first group increase (as far as the absolute value is concerned) with the hydrogen bond formation, and the monomer relaxation contributes significantly to this effect. The coupling constants of the second group change in the opposite direction and, interestingly, these effects are larger than those on the couplings through bonds directly engaged in the hydrogen bond formation. This suggests that the couplings

TABLE 5: The Calculated Changes in the Intramolecular Spin−Spin Coupling Constants (in Hertz) upon Fa−Fa and Fa−Fi Dimer Formation

			$(\Delta J)_{dim}$	$(\Delta J)_{relax}$	$(\Delta J)_{total}$	BSSE SCF(%)
		^{1}J(NH) coupling				
Fa−Fa	Fa	^{1}J(N3H4)	−1.60	−1.53	−3.14	−4.5
Fa−Fa	Fa	^{1}J(N3H5)	2.09	0.69	2.78	−1.4
Fa−Fi	Fa	^{1}J(N4H7)	−0.43	−1.98	−2.42	8.0
Fa−Fi	Fa	^{1}J(N4H8)	3.60	0.84	4.44	−0.5
Fa−Fi	Fi	^{1}J(N5H10)	−2.12	−1.35	−3.48	−2.7
Fa−Fi	Fi	^{1}J(N5H11)	2.24	0.92	3.16	−0.8
Fa−Fi	Fi	^{1}J(N6H13)	−1.87	−0.64	−2.52	3.0
		^{1}J(CO) coupling				
Fa−Fa	Fa	^{1}J(C1O2)	−3.59	2.59	−0.99	8.9
Fa−Fi	Fa	^{1}J(C1O3)	−1.78	2.66	0.88	7.6
		^{1}J(CN) coupling				
Fa−Fa	Fa	^{1}J(C1N3)	0.11	−1.32	−1.21	2.1
Fa−Fi	Fa	^{1}J(C1N4)	0.10	−1.33	−1.24	0.9
Fa−Fi	Fi	^{1}J(C2N5)	2.03	−1.28	0.75	1.8
Fa−Fi	Fi	^{1}J(C2N6)	−0.92	1.07	0.15	1.7
		^{1}J(CH) coupling				
Fa−Fa	Fa	^{1}J(C1H6)	−2.31	−1.86	−4.17	−5.0
Fa−Fi	Fa	^{1}J(C1H9)	−4.51	−1.65	−6.16	−3.2
Fa−Fi	Fi	^{1}J(C2H12)	−1.85	−1.72	−3.57	−1.1
		^{2}J(NH) coupling				
Fa−Fa	Fa	^{2}J(N3H6)	5.16	0.17	5.33	−0.1
Fa−Fi	Fa	^{2}J(N4H9)	5.71	−0.02	5.70	−0.3
Fa−Fi	Fi	^{2}J(N5H12)	3.38	−0.21	3.17	0.0
Fa−Fi	Fi	^{2}J(N6H12)	−1.36	−0.17	−1.53	0.5
		^{3}J(HH) coupling				
Fa−Fa	Fa	^{3}J(H6H4)	−1.58	1.63	0.05	−0.7
Fa−Fa	Fa	^{3}J(H6H5)	0.82	0.64	1.46	0.4
Fa−Fi	Fa	^{3}J(H9H7)	−2.06	2.08	0.02	−0.1
Fa−Fi	Fa	^{3}J(H9H8)	0.88	0.71	1.59	0.2
Fa−Fi	Fi	^{3}J(H12H10)	−1.21	1.68	0.47	18.6
Fa−Fi	Fi	^{3}J(H12H11)	0.93	0.76	1.69	0.2
Fa−Fi	Fi	^{3}J(H13H12)	−0.20	−0.33	−0.53	0.5

in amino groups react in a differential way to the shifts in electronic density, although not to the changes in the bond lengths: The monomer relaxation effect is smaller for ^{1}J(N3H5) in Fa−Fa or ^{1}J(N4H8) and ^{1}J(N5H11) in Fa−Fi than for the couplings from the first group. The response of the ^{1}J(N6H13) coupling constant of the proton acceptor to the hydrogen bond formation is similar to that of the couplings of the first group: It increases by approximately 2.5 Hz.

The changes in the ^{1}J(CN) couplings are dominated by the monomer relaxation effects. Interestingly, the total complexation effect on ^{1}J(CN) has a different sign for Fi and Fa even when the coupled nitrogen acts as a proton donor in both cases. This is caused by the dominance of positive $(\Delta J)_{dim}$ contribution in the change of ^{1}J(C2N5) in Fi, while for ^{1}J(C1N3) and ^{1}J(C1N4) negative $(\Delta J)_{relax}$ contributions prevail. Effects such as this are difficult to explain, since spin−spin coupling constants are complex phenomena. Frequently the effect observed on the given coupling is caused by some deformations not in the bond in the coupling path but in the nearby bond (see above), in this case in C2N6. The change of ^{1}J(CO) in formamide also has a different sign in the Fa−Fa dimer than in the Fa−Fi dimer. The source of this effect is analogous to that for ^{1}J(CN): $(\Delta J)_{dim}$ and $(\Delta J)_{relax}$ each have the same sign in Fa−Fa and Fa−Fi, but in Fa−Fa, unlike in Fa−Fi, the negative $(\Delta J)_{dim}$ contribution has a larger absolute value.

The last of the one-bond couplings to be discussed here are the ^{1}J(CH) couplings. In this case, the coupled nuclei do not participate in the hydrogen bond formation. However, the changes in ^{1}J(CH) coupling constants are rather considerable. They are presumably caused by the long-range electrostatic

effects, to which ^{1}J(CH) couplings were found to be responsive.[56−58]

The changes in ^{2}J(NH) couplings are included in Table 5 because of their considerable values, dominated by the effect of the electron cloud deformation. The sign of the change is positive when N acts as a proton donor and negative when N acts as a proton acceptor, i.e., in each case the absolute magnitude of the coupling decreases upon complexation (compare Table 2). The sensitivity of ^{2}J(NH) couplings to the intermolecular interactions is confirmed by considerable experimental solvent shifts for these parameters (see Table 2) and makes them attractive as parameters characterizing the hydrogen bonding. However, for the biopolymers most of these couplings will not be present.

The vicinal proton−proton coupling constants ^{3}J(HH) undergo considerable changes as a result of the deformation of the electron cloud $(\Delta J)_{dim}$. For some of them the monomer deformation contribution adds up to the above effect; for the others these two effects nearly annihilate each other, but on the whole the influence of the hydrogen bonding on the ^{3}J(HH) couplings is definitely nonnegligible. It clearly indicates that a change in ^{3}J(HH) should not be automatically interpreted as evidence of the modification in molecular conformation, since the purely electronic effects of intermolecular interactions may also be considerable.

(a) Monomer Relaxation and Counterpoise Correction Effects. The monomer relaxation effects play an important role in the complexation-induced changes of the spin−spin coupling constants. As was already mentioned, in many cases (^{1}J(CO), ^{1}J(CN), some of the ^{3}J(HH) couplings) they dominate the total effect, which contrast with trends for the complexation-induced changes of the shieldings constants (Tables 3 and 4). The basis set superposition error estimated at the SCF level by means of the counterpoise correction technique is small (see last column of Table 5). This allowed us to neglect this issue in the previous discussion of the hydrogen bond formation effects on the individual spin−spin coupling constants.

To sum up, the hydrogen-bond-induced changes in the spin−spin coupling constants are in some cases substantial. ^{1}J(NH) and ^{2}J(NH) couplings in particular seem to be promising as potential hydrogen bond parameters. However, the relative changes of the coupling constants are several times smaller than the effects of the hydrogen bond formation on the shielding constants. Because of this and the problems with measuring the reference spin−spin coupling constants of the noninteracting monomer in biopolymers, we decided to concentrate on the intermolecular hydrogen bond-transmitted coupling constants, for which these problems do not emerge.

Intermolecular Spin−Spin Coupling Constants. The most interesting of the calculated hydrogen-bond-transmitted spin−spin couplings are presented in Figure 2. First, we discuss the ^{2h}J(NN) and ^{1h}J(NH) couplings, then the ^{3h}J(CN) couplings, the ^{2h}J(CH) couplings, and finally the intermolecular proton−proton couplings. Several of these couplings can be related to the experimental results for RNA,[17] DNA,[20] and proteins.[15,16,18,19,23]

The ^{2h}J(NN) and ^{1h}J(NH) couplings in the Fa−Fi dimer are generally in agreement with experiment: Their signs and magnitudes are reproduced correctly. Our values are slightly higher than those measured in nucleic base pairs (ca. 6.7 Hz for the U−A pair in RNA[17] and 1.8−3.6 Hz in DNA),[20] but it should be kept in mind that (a) the calculations were carried out for model compounds and (b) MP2 method tends to give too short hydrogen bond lengths, which results in overestimated hydrogen-bond transmitted couplings (see below).

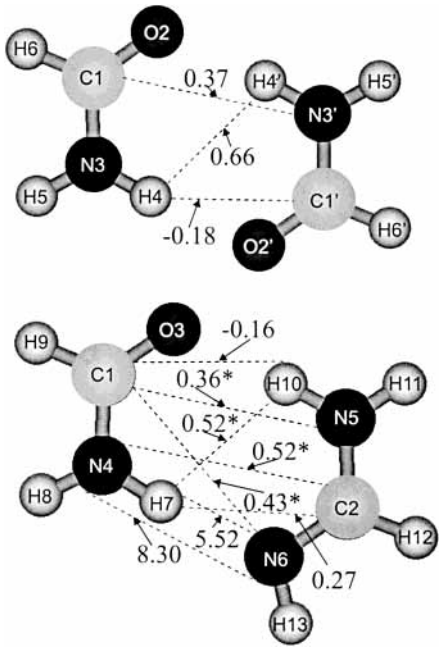

Figure 2. The hydrogen bond-transmitted coupling constants for the optimized structures of Fa−Fa dimer and Fa−Fi dimer. The asterisk indicates no SD term.

Our results indicate that the ^{3h}J(CN) couplings should have positive signs. This contradicts the experiment, which sheds doubt on the accuracy of our calculations. However, we believe that the question of the sign of ^{3h}J(CN) is still open, since the sign assignment in ref 19 was not straightforward. The absolute magnitude of ^{3h}J(CN) is in fair agreement with experiment (ca. 0.37 ± 0.15 for α-helix[15,16]).

According to our knowledge there is only one experimental work reporting interresidual ^{2h}J(CH) couplings.[23] The calculated values are slightly discrepant with those communicated there (ca. 0.4−0.6 Hz, sign not given). Our calculations indicate that ^{2h}J(CH) couplings are positive for N−H···N═C bonds and negative for N−H···O═C bonds. However, these results are not conclusive, since the small values of the ^{2h}J(CH) couplings make them difficult not only to measure but also to calculate accurately.

The intermolecular hydrogen-bond-transmitted couplings between protons engaged in the nearby hydrogen bonds (here ^{h}J(H4H4′) in Fa−Fa and ^{h}J(H4H10) in Fa−Fi) have not been detected experimentally. Our results indicate that these couplings should have measurable values, although they are smaller than that calculated for the $(HCOOH)_2$ dimer.[35]

Now we shall discuss the contributions of different terms to the hydrogen-bond-transmitted coupling constants. The largest ^{2h}J(NN) coupling is determined practically exclusively by its Fermi contact term, since other terms are 2 orders of magnitude smaller. In the case of ^{1h}J(NH) the dia- and paramagnetic spin−orbit terms are not negligible (−0.4 and 0.3 Hz, respectively), but their signs are opposite and they cancel each other. The SD term of 0.03 Hz is insignificant. ^{3h}J(CN) couplings are also dominated by the FC term. In contrast to them, the intermolecular proton−proton coupling constants are determined mainly by the PSO and DSO terms, the FC term being small (approximately −0.1 Hz) and practically annihilating with the SD term. In the intermolecular ^{2h}J(CH) couplings all terms contribute equally significantly. The difference in sign between ^{2h}J(C1H4′), ^{2h}J(C1H10) and ^{2h}J(C2H7) origins from mutual canceling of large (0.48 Hz and −0.41 Hz) DSO and PSO terms and the SD term of −0.10 Hz in ^{2h}J(C2H7) leaving out the

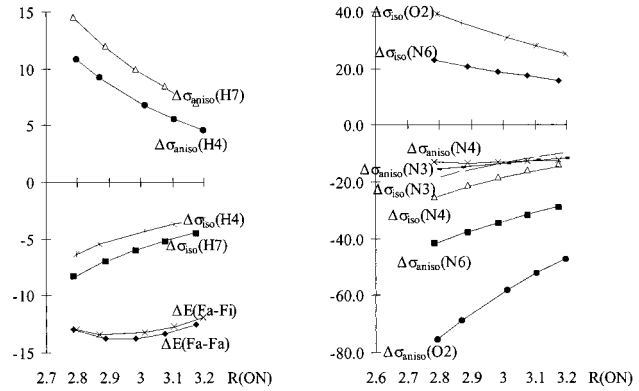

Figure 3. (a) The dependence of changes in the ^{1}H shielding constants (in ppm) and the interaction energy (in kcal/mol) on the intermolecular R(ON) distance (in angstroms). (b) The dependence of changes in the ^{17}O and ^{15}N shielding constants (in parts per million) on the intermolecular R(ON) distance (in angstroms).

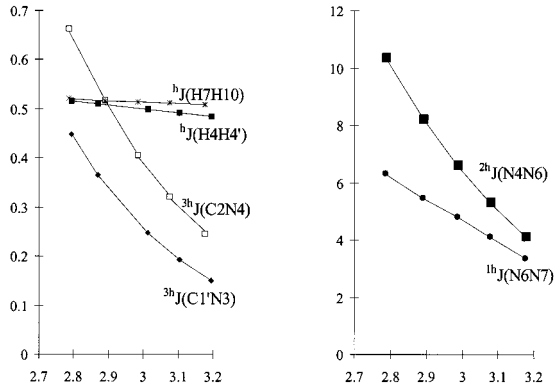

Figure 4. (a) The dependence of the hydrogen bond-transmitted ^{3h}J(CN) and ^{h}J(HH) coupling constants (in Hertz) on the intermolecular R(ON) distance (in angstroms). (b) The dependence of the hydrogen bond-transmitted ^{1h}J(NH) and ^{2h}J(NN) coupling constants (in Hz) on the intermolecular R(ON) distance (in angstroms).

positive FC term (0.30 Hz), while in the remaining coupling the sign is determined by the largest PSO term.

Dependence of the NMR Parameters on the Hydrogen Bond Length. In this section we discuss the dependence of the calculated NMR shielding constants and the intermolecular spin−spin coupling constants on the hydrogen bond length. To establish this dependence, the calculations were carried out for five intermolecular distances for Fa−Fa and Fa−Fi dimers, keeping fixed the optimized internal geometry of the dimers.

Changes of the Shielding Constants. The dependence of selected isotropic shielding constants and shielding anisotropies on the intermolecular R(ON) distance in Fa−Fa and Fa−Fi dimers together with the interaction energy are visualized in Figure 3. The changes of the shielding constants of the protons engaged in the NH···Y hydrogen bond are presented in Figure 3a, Y being the O atom in Fa−Fa and the N atom in Fi−Fa. The change in the shielding of the proton H10 in Fa−Fi practically overlaps that of the proton H4 in Fa−Fa, so it is omitted.

The curves for the proton shielding in the N−H···O═C hydrogen bond of Fa−Fa and the N−H···N═C hydrogen bond of Fa−Fi are nearly parallel. This indicates that the type of acceptor influences the net hydrogen bond effect on σ (^{1}H). However, the shape of the dependence of σ (^{1}H) on the intermolecular distance is little affected by the type of the proton acceptor. The dependence of the ^{1}H shielding on the hydrogen bond length is substantial and therefore easy to parametrize, but the direct correlation with the interaction energy does not emerge. This is in agreement with previous theoretical works[11,27,30,35] in which the correlation of ^{1}H shielding with the interaction energy was observed for a range of different hydrogen-bonded complexes[11,35] but not when the intermolecular shielding surface for the individual complex was calculated.[27,30] The change in the ^{1}H shielding anisotropy decreases even more steeply with the intermolecular distance than the change in the ^{1}H isotropic shielding. It makes the former a very suitable parameter characterizing the hydrogen bond.

Now we shall discuss the changes in the isotropic shieldings and the shielding anisotropies of the proton acceptors (O2′ in Fa−Fa and N6 in Fa−Fi) and the proton donors (N3 in Fa−Fa and N4 in Fa−Fi) visualized in Figure 3b as functions of the intermolecular distance. The change in the ^{17}O shielding constant of Fa in Fa−Fi is not visualized in Figure 3b, since for all intermolecular distances it is similar to the change of the ^{17}O shielding constant of Fa in Fa−Fa. The ^{15}N shielding constant of N5 in Fa−Fi is not included, either, for the same reason.

The dependence of the isotropic and anisotropic ^{17}O shielding of the proton acceptor on the hydrogen bond length is steep. The variation of the proton acceptor ^{15}N shielding with the intermolecular distance is similar to that of the ^{17}O shielding, although proportionally smaller. The dependence of all the proton donor isotropic shieldings and shielding anisotropies on the hydrogen bond length seems to be nearly linear. This we attribute to a small number of calculated points, since the previous calculations clearly show the nonlinearity of this dependence.[27]

The changes of the isotropic shielding of the proton donor vary similarly with the distance for all atoms under study. In contrast to that, the ^{15}N shielding anisotropy of the proton donor atom changes more slowly with the intermolecular distance when the acceptor is another nitrogen atom (the shielding anisotropy of N4 in Fa−Fi) than when oxygen atom is the acceptor (the shielding anisotropy of N3 in Fa−Fa or of N5 in Fa−Fi). The dependence of the proton acceptor shieldings on the intermolecular distance is monotonic, with one exception: The shielding anisotropy of N4 in Fa−Fi exhibits a minimum near the energy minimum.

The changes of the carbonyl isotropic ^{13}C shielding with the hydrogen bond length (not shown in Figure 3) are relatively slow. The slope of this dependence is in approximate agreement with the empirical correlations for peptides.[59] The dependence of ^{13}C shielding anisotropy on R is more steep, which indicates that it is a better hydrogen bond parameter.

The Intermolecular Spin−Spin Coupling Constants. Figure 4 visualizes the dependence of the selected hydrogen-bond-transmitted couplings in Fa−Fa (^{3h}J(C1N3′), ^{h}J(H4H4′)), and Fa−Fi (^{3h}J(C2N4), ^{h}J(H7H10), ^{2h}J(N4N6), ^{1h}J(N6H7)) on the intermolecular distance R(ON). The remaining ^{3h}J(CN) couplings depend on the intermolecular distance analogously to ^{3h}J(C1N3′) and ^{3h}J(C2N4), so they are not shown in Figure 4.

Three types of dependence of the hydrogen bond-transmitted coupling constant on the intermolecular distance can be distinguished: fast exponential decay of the ^{3h}J(CN), ^{1h}J(NH) and ^{2h}J(NN) couplings, slow decrease of the carbon-proton couplings, and even slower decrease of the proton−proton couplings with increase of R. This variety can be explained by analysis of the distance dependence of individual contributions to these couplings. ^{3h}J(CN), ^{1h}J(NH), and ^{2h}J(NN) couplings are dominated by the FC term, which decreases fast with increase in the distance between the coupled nuclei. The DSO and PSO terms, which are the most significant contributions to the ^{h}J(HH) couplings, are less distance dependent. The ^{2h}J(CH) couplings

represent an intermediate case. The sensitivity of the ^{1h}J(NH) and ^{2h}J(NN) couplings, the latter in particular, to the hydrogen bond length makes them very attractive as parameters for characterization of hydrogen bonds.

Concluding Remarks

Calculations of the NMR shielding constants and the scalar spin−spin coupling constants, both intra- and intermolecular, were carried out for formamide−formamide and formamidine-formamidine dimers by using the MCSCF method for the calculations of the spin−spin couplings and MP2 for the calculations of the shielding constants. The general conclusions for the calculated NMR shielding constants and then for the spin−spin coupling constants are summarized below, followed by the methodological conclusions.

General Conclusions. The changes in the shielding constant of the proton engaged in the N−H···Y hydrogen bond formation depend predominantly on the type of proton acceptor Y. The same observation is made for the ^{15}N shieldings of the proton donor atoms. The changes in the shielding constants of the proton acceptors Y are the largest and depend most steeply on the hydrogen bond length. The dependence of the shielding constants under study on the hydrogen bond length is monotonic in the range investigated, with the exception of the ^{15}N shielding anisotropy of formamide nitrogen in the Fa−Fi dimer.

The ^{1}J(NH) intramolecular couplings are found to increase under the influence of the hydrogen bond when the coupled proton is engaged in it and decrease substantially in the case of the coupling through an adjacent bond in amino group. The changes in ^{1}J(CN) are not significant and are difficult to analyze, since they are the outcome of a subtle balance between the effects of electron cloud deformation and monomer relaxation effects. The ^{2}J(NH) couplings are more promising as potential hydrogen bond parameters. The hydrogen bond formation also considerably influences the ^{1}J(CH) couplings and some of the ^{3}J(HH) couplings.

The calculation of hydrogen-bond transmitted coupling constants for Fa−Fi dimer with the optimized structure yields ^{1h}J(NH) = 5.5 Hz and ^{2h}J(NN) = 8.3 Hz. This is in approximate agreement with the experimental results for nucleic acids. The magnitude of the calculated ^{3h}J(CN) couplings (approximately 0.4 Hz) is in agreement with the experiment, but the sign is opposite. The calculated values for the ^{2h}J(CH) couplings seem to be underestimated. Our calculations predict that the couplings between protons engaged in adjacent hydrogen bonds should have measurable values. The discussed hydrogen-bond-transmitted couplings are dominated by the Fermi contact terms, with the exception of the proton−proton couplings, where the noncontact spin−orbit terms prevail. This affects their dependence on the hydrogen bond length: The hydrogen-bond-transmitted couplings dominated by the FC term decrease fast when the hydrogen bond length is increased, in contrast to those dominated by the spin−orbit terms.

Methodological Conclusions. The proton shielding constants calculated at the SCF level are in agreement with the MP2 results—both their absolute values and their hydrogen bond-induced changes. The most significant differences between MP2 and SCF results are found for the ^{17}O shielding constants in the C═O group and the ^{15}N shielding constant in the HN═C group. These difficult cases probably require post-MP2 correlation treatment. The MCSCF method performs better for them.

The basis set superposition error for the changes of the shielding constants is small for the basis set employed and is of comparable magnitude at the MP2 and SCF levels. The monomer relaxation effects are not very important for the changes of the shielding constants, with the exception of the relatively small changes in ^{13}C shieldings.

The basis set superposition error estimated at the SCF level is not significant for the coupling constants. The monomer relaxation effects contribute significantly to the hydrogen-bond-induced changes of the intramolecular coupling constants, in some cases dominating them.

Acknowledgment. We acknowledge the support from the 3TO9A12116 KBN grant, NSF grants 9805465 and 9706268, and ONR grant N00014-98-0592.

References and Notes

(1) Wu, Z. R.; Ebrahimian, S.; Zawrotny, M. E.; Thornburg, L. D.; Perez-Alvarado, G. C.; Brothers, P.; Pollack, R. M.; Summers, M. F. *Science* **1997**, *276*, 415.
(2) Perrin, C. L. *Science* **1994**, *266*, 1665.
(3) Cleland, W. W.; Frey, P. A.; Gertl, J. A. *J. Biol. Chem.* **1998**, *273*, 25529.
(4) Scheiner, S.; Kar, T. *J. Am. Chem. Soc.* **1995**, *117*, 6970.
(5) Guthrie, J. P.; Kluger, R. *J. Am. Chem. Soc.* **1993**, *115*, 11569.
(6) Waeshel, A.; Papazyan, A.; Kollman, P. A. *Science* **1995**, *269*, 103.
(7) Gertl, J. A.; Gassman, P. G. *J. Am. Chem. Soc.* **1994**, *115*, 11552.
(8) Del Bene, J. E.; Perera, S. A.; Bartlett, R. J. *J. Phys. Chem. A* **1999**, *103*, 8121.
(9) Frey, P. A.; Whitt, S. A.; Tobin, J. B. *Science* **1994**, *264*, 1927.
(10) Brunner, E.; Strenberg, U. *Prog. NMR. Spectrosc.* **1998**, *32*, 21.
(11) Kumar, G. A.; McAllister, M. A. *J. Org. Chem.* **1998**, *63*, 6968.
(12) Sitkoff, D.; Case, D. A. *Prog. Nucl. Magn. Resonan. Spectrosc.* **1998**, *32*, 165.
(13) LiWang, A. C.; Bax, A. *J. Magn. Reson.* **1999**, *127*, 54.
(14) Juranic, N.; Ilich, P. K.; Macura, S. *J. Am. Chem. Soc.* **1995**, *117*, 405.
(15) Cordier, F.; Grzesiek, S. *J. Am. Chem. Soc.* **1999**, *121*, 1601.
(16) Cornilescu, G.; Hu, J.-S.; Bax, A. *J. Am. Chem. Soc.* **1999**, *121*, 2949.
(17) Dingley, A. J.; Grzesiek, S. *J. Am. Chem. Soc.* **1998**, *120*, 8293.
(18) Blake, P. R.; Park, J. B.; Adams, M. W. W.; Summers, M. F. *J. Am. Chem. Soc.* **1992**, *114*, 4931.
(19) Cornilescu, G.; Ramirez, B. E.; Frank, M. K.; Marius Clore, G.; Gronenborn, A. M.; Bax, A. *J. Am. Chem. Soc.* **1999**, *121*, 6275.
(20) Dingley, A. J.; Masse, J. E.; Peterson, R. D.; Barfield, M.; Feigon, J.; Grzesiek, S. *J. Am. Chem. Soc.* **1999**, *121*, 6019.
(21) Shenderovich, I. G.; Smirnov, S. H.; Denisov, G. S.; Gindin, V. A.; Golubev, N. S.; Dunger, A.; Reibke, R.; Kirpekar, S.; Malkina, O. L.; Limbach, H.-H. *Ber. Bunsen-Ges. Phys. Chem.* **1998**, *102*, 422.
(22) Golubev, N. S.; Shenderovich, I. G.; Smirnov, S. H.; Denisov, G. S.; Limbach, H.-H. *Chem.—Eur. J.* **1999**, *5*, 492.
(23) Cordier, F.; Rogowski, M.; Grzesiek, S.; Bax, A. *J. Magn. Reson.* **1999**, *140*, 510.
(24) Helgaker, T.; Jaszuński, M.; Ruud, K. *Chem. Rev.* **1999**, *99*, 293.
(25) Fukui, H. *Prog. Nucl. Magn. Spectrosc.* **1999**, *35*, 267.
(26) Fukui, H. *Prog. Nucl. Magn. Spectrosc.* **1997**, *31*, 317.
(27) Ditchfield, R. *J. Chem. Phys.* **1976**, *65*, 3123.
(28) McMichael Rohlfing, C.; Allen, L. C.; Ditchfield, R. *Chem. Phys. Lett.* **1982**, *86*, 380.
(29) McMichael Rohlfing, C.; Allen, L. C.; Ditchfield, R. *J. Chem. Phys.* **1983**, *79*, 4958.
(30) Chesnut, D. B.; Rusiloski, B. E. *J. Phys. Chem.* **1993**, *97*, 2839.
(31) Janoschek, R. *Mol. Phys.* **1996**, *89*, 1301.
(32) Hinton, J. F.; Wolinski, K. Ab initio GIAO Magnetic Shielding Tensor for Hydrogen Bonded Systems. In *Theoretical Treatments of Hydrogen Bonding*; Hadzi, D., Ed.; Wiley & Sons: New York 1997.
(33) Perera, S. A.; Bartlett, R. J. *J. Am. Chem. Soc.* **2000**, *122*, 1231.
(34) Scheurer, C.; Brüschweiler, R. *J. Am. Chem. Soc.* **1999**, *121*, 8661.
(35) Pecul, M.; Leszczynski, J.; Sadlej, J. *J. Chem. Phys.* **2000**, *112*, 7930.
(36) Pecul, M.; Sadlej, J. *Chem. Phys. Lett.* **1999**, *308*, 486.
(37) Benedict, H.; Shenderovich, I. G.; Malkina, O. L.; Malkin, V. G.; Denisov, G. S.; Golubev, N. S.; Limbach, H.-H. *J. Am. Chem. Soc.* **2000**, *112*, 1979.
(38) Malkin, V. G.; Malkina, O. L.; Salahub, D. R. *Chem. Phys. Lett.* **1994**, *221*, 91.
(39) Malkina, O. L.; Salahub, D. R.; Malkin, V. G. *J. Chem. Phys.* **1996**, *105*, 8793.
(40) Vahtras, O.; Ågren, H.; Jørgensen, P.; Helgaker, T.; Jensen, H. J. Aa. *Chem. Phys. Lett.* **1993**, *209*, 201.

(41) Ghanty, T. K.; Staroverov, V. N.; Koren, P. R.; Davidson, E. R. *J. Am. Chem. Soc.* **2000**, *122*, 1210.

(42) Zhanpeisov, N.; Leszczynski, J. *J. Phys. Chem. A* **1999**, *103*, 8317.

(43) Sponer, J.; Hobza, P. *Chem. Phys. Lett.* **1997**, *267*, 263.

(44) Sponer, J.; Hobza, P. *J. Phys. Chem. A* **2000**, *104*, 4592.

(45) Vaara, J.; Kaski, J.; Jokisaari, J.; Diehl, P. *J. Phys. Chem. A* **1997**, *101*, 5069. Vaara, J.; Kaski, J.; Jokisaari, J.; Diehl, P. *J. Phys. Chem. A* **1997**, *101*, 9185.

(46) Boys, S. F.; Bernardi, F. *Mol. Phys.* **1970**, *19*, 553.

(47) Xanteas, S. S. *J. Chem. Phys.* **1996**, *104*, 8821.

(48) Frisch, M. J.; Trucks, G. W.; Schlegel, H. B.; Scuseria, G. E.; Robb, M. A.; Cheeseman, J. R.; Zakrzewski, V. G.; Montgomery, J. A., Jr.; Stratmann, R. E.; Burant, J. C.; Dapprich, S.; Millam, J. M.; Daniels, A. D.; Kudin, K. N.; Strain, M. C.; Farkas, O.; Tomasi, J.; Barone, V.; Cossi, M.; Cammi, R.; Mennucci, B.; Pomelli, C.; Adamo, C.; Clifford, S.; Ochterski, J.; Petersson, G. A.; Ayala, P. Y.; Cui, Q.; Morokuma, K.; Malick, D. K.; Rabuck, A. D.; Raghavachari, K.; Foresman, J. B.; Cioslowski, J.; Ortiz, J. V.; Stefanov, B. B.; Liu, G.; Liashenko, A.; Piskorz, P.; Komaromi, I.; Gomperts, R.; Martin, R. L.; Fox, D. J.; Keith, T.; Al-Laham, M. A.; Peng, C. Y.; Nanayakkara, A.; Gonzalez, C.; Challacombe, M.; Gill, P. M. W.; Johnson, B.; Chen, W.; Wong, M. W.; Andres, J. L.; Gonzalez, C.; Head-Gordon; M. GAUSSIAN 98 Revision a.6; Gaussian, Inc.: Pittsburgh, PA, 1998.

(49) Vahtras, O.; Ågren, H.; Jørgensen, P.; Jensen, H. J. Aa.; Padkjær, S. B.; Helgaker, T. *J. Chem. Phys.* **1992**, *96*, 6120.

(50) Helgaker, T.; Jensen, H. J. Aa.; Jørgensen, P.; Olsen, J.; Ruud, K.; Ågren, H.; Andersen, T.; Bak, K. L.; Bakken, V.; Christiansen, O.; Dahle, P.; Dalskov, E. K.; Enevoldsen, T.; Fernandez, B.; Heiberg, H.; Hettema, H.; Jonsson, D.; Kirpekar, S.; Kobayashi, R.; Koch, H.; Mikkelsen, K. V.; Norman, P.; Packer, M. J.; Saue, T.; Taylor, P. R.; Vahtras, O. Dalton: an ab initio Electronic Structure Program Release 1.0, 1997. See http://www.kjemi.uio.no/software/dalton/dalton.html.

(51) Dunning, T. H., Jr. *J. Chem. Phys.* **1989**, *90*, 1007.

(52) Kendall, R. A.; Dunning, T. H., Jr.; Harrison, R. J. *J. Chem. Phys.* **1992**, *96*, 6796.

(53) Helgaker, T.; Jaszuński, M.; Ruud, K.; Górska, A. *Theor. Chim. Acc.* **1998**, *99*, 175.

(54) Pecul, M.; Leszczynski, J. Unpublished results.

(55) Ferchiou, S.; Giessner-Prettre, C. *J. Magn. Reson.* **1985**, *61*, 262.

(56) Vizioli, C.; de Azúa, M. C. R.; Giribet, C. G.; Contreras, R. H.; Turi, L.; Danenberg, J. J.; Rae, I. D.; Weigold, J. A.; Malagoli, M.; Zanasi, R.; Lazzeretti, P. *J. Phys. Chem.* **1994**, *98*, 8858.

(57) Afonin, A. V.; Vizioli, C.; de Azúa, M. C. R.; Contreras, R. H. *Russ. Chem. Bull.* **1996**, *45*, 1292.

(58) Pecul, M.; Sadlej, J. *Chem. Phys.* **1999**, *248*, 27.

(59) Tsuchiya, K.; Takahashi, A.; Takeda, N.; Asakawa, N.; Kuroki, S.; Ando, I.; Shoji, A.; Ozaki, T. *J. Mol. Struct.* **1995**, *350*, 233.